



Universiteit
Leiden
The Netherlands

Non-decoupling of heavy scalars in cosmology

Hardeman, A.R.

Citation

Hardeman, A. R. (2012, June 8). *Non-decoupling of heavy scalars in cosmology. Casimir PhD Series*. Retrieved from <https://hdl.handle.net/1887/19062>

Version: Corrected Publisher's Version

License: [Licence agreement concerning inclusion of doctoral thesis in the Institutional Repository of the University of Leiden](#)

Downloaded from: <https://hdl.handle.net/1887/19062>

Note: To cite this publication please use the final published version (if applicable).

Cover Page



Universiteit Leiden



The handle <http://hdl.handle.net/1887/19062> holds various files of this Leiden University dissertation.

Author: Hardeman, Sjoerd Reimer

Title: Non-decoupling of heavy scalars in cosmology

Date: 2012-06-08

CHAPTER 5

Two-field models of inflation

5.1 Introduction

In the previous chapter we developed a framework, extending Groot Nibbelink and van Tent (2000, 2002), in which we can calculate the effects of turning field space trajectories on its perturbations. In this chapter, we will use that framework to calculate features in the inflationary power spectrum generated by a turn in the inflaton trajectory. Furthermore, we will derive an effective field theory that is valid for the large hierarchy limit $m_H \gg H$, and show that also in this limit there can be significant features. As we will shortly demonstrate, the parameter determining how relevant a local turn in the background inflaton trajectory is for the effective dynamics of the adiabatic mode is given by the departure from unity of the quantity $e^\beta = 1 + 4\dot{\phi}_0^2/(\kappa^2 M^2)$, where $\dot{\phi}_0$ is the speed of the inflaton background field, κ is the radius of curvature of the curve in field space and M is the mass of the direction normal to the trajectory. Keeping in mind that during slow-roll inflation, the inflaton velocity is given by $\dot{\phi}_0 = \sqrt{2\epsilon} M_{\text{Pl}} H$, with ϵ being the usual slow-roll parameter, it follows that $e^\beta = 1 + 8\epsilon M_{\text{Pl}}^2 H^2/(\kappa^2 M^2)$. Thus, even with $M^2 \gg H^2$, if the radius of curvature describing the turn is small enough, significant imprints of heavy physics on the dynamics of the adiabatic mode can arise. More generally, whenever $e^\beta \neq 1$, some amount of particle creation takes place that backreacts on the dynamics of the adiabatic mode. Let us not forget that in addition to the scale invariance of the power spectrum, single-field slow-roll inflation predicts that the observed CMB temperature anisotropies seeded by the curvature perturbation satisfy Gaussian statistics to a high degree of accuracy (Maldacena, 2003).

Interestingly, in the class of models examined in this work, if the normal direction to the inflaton trajectory is sufficiently massive ($M^2 \gg H^2$), it is possible to compute an effective action for the adiabatic mode capturing the relevant operators of the full multi-field dynamics. This effective theory has the characteristic that the adiabatic mode propagates with a speed of sound given by

$$c_s^2 = e^{-\beta} \tag{5.1}$$

and therefore becomes a functional of (the curvature of) the trajectory traversed by the inflaton (as discussed in the previous chapter). Interestingly, this result has as a special case the particular context of Tolley and Wyman (2010) and indicates the presence of non-Gaussian signatures correlated with features in the power spectrum.¹

This chapter will start with a discussion of two field models for inflation, generalising the discussion of section 4.4. In this section, we will also derive the appropriate expressions for the power spectrum. In the next section, section 5.3, we will derive a single-field effective theory with a reduced speed of sound, where the speed of sound is determined by turns in the direction of the field that is integrated out. Then, we will derive the two-field equations of motion in the limit of slow-roll inflation. We conclude this section by showing that the effective field theory can also be found in the traditional way (Rubin, 2001). Next, in section 5.4 we solve the equations of motion for specific trajectories with turns, and show that this leads to oscillations in the power spectrum. We also perform the calculation in the effective single-field theory with a reduced speed of sound, and see that for the large hierarchy limit both methods agree. This leads to the conclusion that the effect of a turn in field space is signalled by a simultaneous appearance of oscillations in the power spectrum and nongaussianities, as is explained in section 5.5

5.2 Inflationary models with two scalar fields

We now study the evolution of perturbations in systems containing only two relevant scalar fields. In this case, it is always possible to take the set of vielbeins $\{e_I^a\}$ to consist entirely in $e_T^a = T^a$ and $e_N^a = N^a$ defined in Section 4.2.1. Then, the projection tensor P_{ab} introduced in (eq. 4.23) vanishes identically and one is left with the

¹In the paper by Cremonini et al. (2010b) the parametrisation of the non-decoupling parameter of the isocurvature directions ξ relates as a specific realisation of our analysis. This is easiest seen through comparing expressions (23) in Cremonini et al. (2010b) with (eq. 5.37) or (eq. 5.60) here.

relations

$$\frac{DT^a}{dt} = -H\eta_\perp N^a, \quad (5.2)$$

$$\frac{DN^a}{dt} = H\eta_\perp T^a. \quad (5.3)$$

At this point we notice that the normal vector N^a has always the same orientation with respect to the curved trajectory, which is due to the presence of the signature function s_N in (eq. 4.9). For definiteness, let us agree that the normal direction N^a has a right-handed orientation with respect to T^a as shown in Figure 5.1. With this

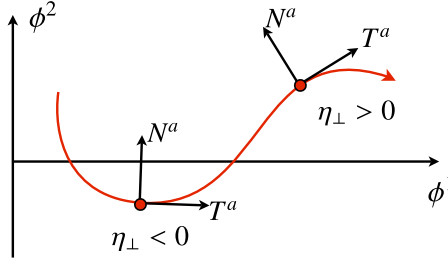


Figure 5.1: The figure shows a fixed right-handed orientation of N^a with respect to T^a . If the turn is towards the left then η_\perp is negative, whereas if the turn is towards the right then η_\perp is positive.

convention η_\perp changes signs smoothly in such a way that if the turn is towards the left then η_\perp is negative, whereas if the turn is towards the right then η_\perp is positive. A concrete choice for T^a and N^a with these properties is:

$$T^a = \frac{1}{\dot{\phi}_0} (\dot{\phi}^1, \dot{\phi}^2), \quad (5.4)$$

$$N^a = \frac{1}{\dot{\phi}_0 \sqrt{\gamma}} (-\gamma_{22}\dot{\phi}^2 - \gamma_{12}\dot{\phi}^1, \gamma_{11}\dot{\phi}^1 + \gamma_{21}\dot{\phi}^2), \quad (5.5)$$

where $\gamma = \gamma_{11}\gamma_{22} - \gamma_{12}\gamma_{21}$ is the determinant of γ_{ab} . To continue, parallel and normal perturbations with respect to the inflationary trajectory are then given by

$$v^T = a Q^T = a T_a Q^a, \quad (5.6)$$

$$v^N = a Q^N = a N_a Q^a. \quad (5.7)$$

By choosing this frame, one finds that $Z_{TN} = -Z_{NT} = aH\eta_{\perp}$. The coupled equations of motion describing the evolution of both modes $v_{\alpha}^T(k, \tau)$ and $v_{\alpha}^N(k, \tau)$ become

$$\frac{d^2 v_{\alpha}^T}{d\tau^2} + 2\zeta \frac{dv_{\alpha}^N}{d\tau} - \zeta^2 v_{\alpha}^T + \frac{d\zeta}{d\tau} v_{\alpha}^N + \Omega_{TN} v_{\alpha}^N + (\Omega_{TT} + k^2) v_{\alpha}^T = 0, \quad (5.8)$$

$$\frac{d^2 v_{\alpha}^N}{d\tau^2} - 2\zeta \frac{dv_{\alpha}^T}{d\tau} - \zeta^2 v_{\alpha}^N - \frac{d\zeta}{d\tau} v_{\alpha}^T + \Omega_{NT} v_{\alpha}^T + (\Omega_{NN} + k^2) v_{\alpha}^N = 0, \quad (5.9)$$

where we have defined

$$\zeta \equiv Z_{TN} = aH\eta_{\perp}. \quad (5.10)$$

In the previous equations, the symmetric matrix Ω_{IJ} is defined in (eq. 4.36) and (eq. 4.48) and consists of the following elements:

$$\Omega_{TT} = -a^2 H^2 (2 + 2\epsilon - 3\eta_{\parallel} + \eta_{\parallel} \xi_{\parallel} - 4\epsilon \eta_{\parallel} + 2\epsilon^2 - \eta_{\perp}^2), \quad (5.11)$$

$$\Omega_{NN} = -a^2 H^2 (2 - \epsilon) + a^2 M^2, \quad (5.12)$$

$$\Omega_{TN} = a^2 H^2 \eta_{\perp} (3 + \epsilon - 2\eta_{\parallel} - \xi_{\perp}), \quad (5.13)$$

where $M^2 \equiv V_{NN} + H^2 M_{\text{pl}}^2 \epsilon \mathbb{R}$ is the effective squared mass of the v^N -mode and $\mathbb{R} = 2\mathbb{R}_{TNTN} = T^a N^b T^c N^d \mathbb{R}_{abcd}$ is the Ricci scalar parametrising the geometry of \mathcal{M} . Furthermore, ξ_{\parallel} was defined in (eq. 4.31) and additionally we have defined²

$$\xi_{\perp} \equiv -\frac{\dot{\eta}_{\perp}}{H\eta_{\perp}}. \quad (5.14)$$

To arrive at the form of the mass matrix Ω_{IJ} shown in (eq. 5.11), (eq. 5.12) and (eq. 5.13), we may start from the explicit form deduced out of (eq. 4.36) and (eq. 4.48) for the case of two-field models,

$$\Omega_{TT} = -a^2 H^2 (2 - \epsilon) + a^2 V_{\phi\phi} - 2a^2 H^2 \epsilon (3 - 2\eta_{\parallel} + \epsilon), \quad (5.15)$$

$$\Omega_{NN} = -a^2 H^2 (2 - \epsilon) + a^2 V_{NN} + a^2 H^2 M_{\text{pl}}^2 \epsilon \mathbb{R}, \quad (5.16)$$

$$\Omega_{TN} = a^2 V_{\phi N} + 2a^2 H^2 \eta_{\perp} \epsilon, \quad (5.17)$$

where we have defined

$$V_{\phi\phi} \equiv T^a T^b \nabla_a V_b, \quad (5.18)$$

$$V_{NN} \equiv N^a N^b \nabla_a V_b, \quad (5.19)$$

$$V_{\phi N} \equiv T^a N^b \nabla_a V_b. \quad (5.20)$$

²Note that this definition for ξ_{\perp} is different from the definition used in Groot Nibbelink and van Tent (2000, 2002).

Additionally $\mathbb{R} = 2\mathbb{R}_{TNTN} = T^a N^b T^c N^d \mathbb{R}_{abcd}$ is the Ricci scalar parametrising the geometry of \mathcal{M} . Notice that $V_{\phi\phi}$ can be rewritten in the following way:

$$\begin{aligned} V_{\phi\phi} &= T^a \nabla_a (T^b V_b) - T^a (\nabla_a T^b) V_b \\ &= \nabla_\phi V_\phi - \frac{1}{\dot{\phi}_0} \frac{DT^b}{dt} V_b \\ &= \nabla_\phi V_\phi + H^2 \eta_\perp^2, \end{aligned} \quad (5.21)$$

where, to go from the second to the third line we made use of (eq. 5.2) and relation $V_N = \dot{\phi}_0 H \eta_\perp$ coming from the definition of η_\perp in (eq. 4.18). Similarly, the quantity $V_{\phi N}$ may be manipulated as follows:

$$\begin{aligned} V_{\phi N} &= T^a \nabla_a (N^b V_b) - T^a (\nabla_a N^b) V_b \\ &= \nabla_\phi V_N - \frac{1}{\dot{\phi}_0} \frac{DN^b}{dt} V_b \\ &= \nabla_\phi V_N - \frac{H \eta_\perp}{\dot{\phi}_0} V_\phi, \end{aligned} \quad (5.22)$$

where again, to go from the second to the third line, we made use of (eq. 5.2). As a final step, we may use $V_N = \dot{\phi}_0 H \eta_\perp$ to deduce

$$\nabla_\phi V_N = \frac{1}{\dot{\phi}_0} \frac{d}{dt} (\dot{\phi}_0 H \eta_\perp) = -H^2 \eta_\perp (\eta_\parallel + \epsilon + \xi_\perp). \quad (5.23)$$

Collecting all of these terms back into (eq. 5.15), (eq. 5.16) and (eq. 5.17) we finally arrive at (eq. 5.11), (eq. 5.12) and (eq. 5.13). Observe that we are not able to rewrite $V_{NN} = N^a N^b \nabla_a V_b$ in a similar way, since it involves second variations away from the inflationary trajectory. This simply means that the quantity V_{NN} must be regarded as an additional parameter of the model related to the mass of the transverse mode with respect to the inflaton trajectory.

5.2.1 Power spectrum

Expressions (eq. 5.8) and (eq. 5.9) consist of the equations of motion necessary to deduce the generation of the curvature perturbation in the case of two-field inflation. Once the solutions of the fields $v^T = a Q^T$ and $v^N = a Q^N$ are known, it is possible to

define the curvature and isocurvature perturbations as

$$\mathcal{R} \equiv \frac{H}{\dot{\phi}_0} Q^T, \quad (5.24)$$

$$\mathcal{S} \equiv \frac{H}{\dot{\phi}_0} Q^N, \quad (5.25)$$

respectively. Using equation (eq. 4.74) with $I = J = T$, the resulting power spectrum for adiabatic modes are found to be

$$\mathcal{P}_{\mathcal{R}}(k, \tau) = \frac{H^2}{\dot{\phi}_0^2} \mathcal{P}_Q^{TT}(k, \tau) = \frac{k^3}{4\pi^2 a^2 M_{\text{Pl}}^2 \epsilon} \sum_{\alpha=1,2} v_{\alpha}^T(k, \tau) v_{\alpha}^{T*}(k, \tau), \quad (5.26)$$

where a and $\epsilon = \dot{\phi}^2 / (2M_{\text{Pl}}^2 H^2)$ are functions of τ . We can also compute the power spectrum for isocurvature modes and cross correlation as (Gordon et al., 2001, Amendola et al., 2002, Wands et al., 2002)

$$\mathcal{P}_{\mathcal{S}}(k, \tau) = \frac{H^2}{\dot{\phi}_0^2} \mathcal{P}_Q^{NN}(k, \tau), \quad (5.27)$$

$$\mathcal{P}_{\mathcal{RS}}(k, \tau) = \frac{H^2}{\dot{\phi}_0^2} \mathcal{P}_Q^{TN}(k, \tau), \quad (5.28)$$

respectively. They can give rise to observable signatures in the CMB power spectrum (Amendola et al., 2002), but it depends on post-inflationary processes which we do not consider here. In this work we are primarily concerned with the computation of the power spectrum of the curvature perturbation \mathcal{R} at the end of inflation. This corresponds to the quantity

$$\mathcal{P}_{\mathcal{R}}(k) \equiv \mathcal{P}_{\mathcal{R}}(k, \tau_{\text{end}}), \quad (5.29)$$

where τ_{end} is the time at which inflation effectively ends.³ The computations of $\mathcal{P}_{\mathcal{S}}$ and $\mathcal{P}_{\mathcal{RS}}$ can be done in an identical way.

5.2.2 Effective Theory

If a hierarchy of scales is present in the matrix Ω_{IJ} , then we can compute a fairly reliable effective theory out of the system (eq. 5.8) and (eq. 5.9). Indeed, by assuming

³Since in multi-field inflation the adiabatic mode \mathcal{R} (as well as other background quantities) may continue evolving on super horizon scales, here we do not follow the standard practise of evaluating the power spectrum at horizon crossing time $k = aH$ (Gong and Stewart, 2002). See Kinney (2005) for a discussion of this point.

that Ω_{NN} remains positive at all times and that

$$\Omega_{NN} \gg |\Omega_{TT}|, \quad (5.30)$$

$$\Omega_{NN} \gg |\Omega_{TN}|, \quad (5.31)$$

we may integrate the heavy mode v^N out of the system of equations. By examining the specific shape of the entries Ω_{TT} , Ω_{NN} and Ω_{TN} , we see that a generic requisite for this hierarchy to exist is

$$M^2 \gg H^2, \quad (5.32)$$

where M^2 is the effective mass of the heavy mode v^N given by

$$M^2 \equiv V_{NN} + H^2 M_{\text{pl}}^2 \in \mathbb{R}. \quad (5.33)$$

To compute the effective theory we proceed in the same way as in chapter 4. We focus on the mode α associated to slower oscillations due to the hierarchy. Omitting the α label, this mode is necessarily such that

$$\left| \frac{d^2 v^N}{d\tau^2} \right| \ll a^2 M^2 v^N. \quad (5.34)$$

This allows us to disregard the second derivative of v^N in (eq. 5.9), and write v^N in terms of v^T as

$$v^N = \frac{1}{\Omega_{NN} - \zeta^2 + k^2} \left(2\zeta \frac{dv^T}{d\tau} + \frac{d\zeta}{d\tau} v^T - \Omega_{NT} v^T \right). \quad (5.35)$$

This expression for v^N can be inserted back into the remaining equation of motion (eq. 5.8) to obtain an effective equation of motion for the light adiabatic mode v^T . Then, by defining a new field φ as

$$\varphi \equiv e^{\beta/2} v^T, \quad (5.36)$$

$$e^{\beta(\tau, k^2)} \equiv 1 + 4\eta_{\perp}^2 \left(\frac{M^2}{H^2} - 2 + \epsilon - \eta_{\perp}^2 + \frac{k^2}{a^2 H^2} \right)^{-1}. \quad (5.37)$$

we finally arrive at the following effective equation of motion

$$\varphi'' + e^{\beta(\tau, k^2)} k^2 \varphi + \Omega(\tau, k^2) \varphi = 0, \quad (5.38)$$

where the time dependent function $\Omega(\tau, k^2)$ is found to be

$$\Omega(\tau, k^2) = \Omega_0(\tau) - \frac{\beta''}{2} - \left(\frac{\beta'}{2} \right)^2 - aH\beta'(1 + \epsilon - \eta_{\parallel}), \quad (5.39)$$

$$\Omega_0(\tau) = -a^2 H^2 (2 + 2\epsilon - 3\eta_{\parallel} - 4\epsilon\eta_{\parallel} - \xi_{\parallel}\eta_{\parallel} + 2\epsilon^2). \quad (5.40)$$

Notice that Ω_0 is precisely the mass term appearing in the conventional equation of motion for adiabatic fluctuations in single-field slow-roll inflation. Furthermore, we note that in the case where the mass M approaches the cutoff of our theory, our results can be derived from an effective action for the adiabatic mode given by the action

$$S = \frac{1}{2} \int d\tau d^3x \left[\left(\frac{d\varphi}{d\tau} \right)^2 - \nabla\varphi e^{-\beta(\tau, -\nabla^2)} \nabla\varphi - \varphi \Omega(\tau, -\nabla^2) \varphi \right], \quad (5.41)$$

where $\beta(\tau, -\nabla^2)$ and $\Omega(\tau, -\nabla^2)$ are the functions defined in (eqs. 5.37 and 5.39) but with k^2 replaced by $-\nabla^2$. This result corresponds to the generalisation of our previous work, discussed in chapter 4, to the case of a slowly rolling background in the presence of gravity. A slightly more formal deduction of this effective theory may be found in section 5.3.4, where we see that it can be viewed as a leading order effect at the loop level, and as such contains the higher dimensional corrections implied by the general arguments made in Weinberg (2008) and Cheung et al. (2008). In section 5.4 we shall compare the power spectrum obtained using this effective theory with the one obtained from the full set of equations for the perturbations. We anticipate that this effective theory is very reliable regardless of how large the values of β are.

5.3 Slow-roll inflation in two-field models

So far we have not assumed the slow evolution of background quantities. We now proceed to discuss the case of inflation realised in the slow-roll regime, where the scale of inflation H varies slowly. Our main interest is to study the effects appearing from curved inflationary trajectories, where η_\perp is non-vanishing. We will assume that the radius of curvature κ may take values smaller than M_{Pl} , corresponding to turns of the trajectory taking place at field scales smaller than the Planck scale. This situation is certainly allowed and depending on the value of ϵ it may render large values of η_\perp (recall (eq. 4.22) relating η_\perp and κ). By the same token, we will consider models where the normal mode ν^N has a large effective mass $M^2 \gg H^2$.

5.3.1 Slow-roll parameters

In general, given the background equations of motion (eq. 4.6-4.8), we say that a given background quantity A is slowly rolling if its variation satisfies

$$|\delta_A| \equiv \left| -\frac{1}{HA} \frac{dA}{dt} \right| \ll 1. \quad (5.42)$$

Observe that we can write $\epsilon = \delta_H$ and $\eta_{\parallel} = \delta_{\dot{\phi}_0}$, and therefore both H and $\dot{\phi}_0$ evolve slowly if $\epsilon \ll 1$ and $|\eta_{\parallel}| \ll 1$ respectively. Since $\epsilon = \dot{\phi}^2/(2M_{\text{pl}}^2 H^2)$, the condition $|\eta_{\parallel}| \ll 1$ also guaranties that ϵ will remain varying slowly during inflation. It is useful to introduce a single small dimensionless number $\delta \ll 1$ parametrising the slow-roll expansion⁴ and demand that any quantity A to which slow-roll is imposed, generically satisfies

$$\frac{1}{HA} \frac{dA}{dt} = O(\delta), \quad (5.43)$$

which means $\epsilon = O(\delta)$ and $\eta_{\parallel} = O(\delta)$. In the absence of clear evidence of it, for simplicity we shall not consider here hierarchies between different slow-roll parameters. Recall that (eqs. 4.29 and 4.30) are exact equations relating the parameters ϵ , η_{\parallel} and ξ_{\parallel} to the shape of the potential V along the inflationary trajectory. Now, provided that all of these parameters are small, we may re-express these equations to leading order in δ as

$$\eta_{\parallel} + \epsilon = M_{\text{pl}}^2 \frac{\nabla_{\phi} V_{\phi}}{V}, \quad (5.44)$$

$$\epsilon = \frac{M_{\text{pl}}^2}{2} \left(\frac{V_{\phi}}{V} \right)^2. \quad (5.45)$$

These are the usual equations defining the slow-roll parameters in terms of the shape of the first and second derivatives of V .⁵ As long as $\epsilon \ll 1$ and $|\eta_{\parallel}| \ll 1$, the background geometry evolves slowly and the scalar field velocity is determined by the attractor equation of motion $3H\dot{\phi}_0 + V_{\phi} = 0$. For completeness, notice from the definition of η_{\perp} in (eq. 4.18) that it is possible to write $\eta_{\perp} = V_N/(\sqrt{2}\epsilon M_{\text{pl}} H^2)$. Then, using (eq. 5.45) we deduce

$$\eta_{\perp}^2 = 9 \left(\frac{V_N}{V_{\phi}} \right)^2, \quad (5.46)$$

which is valid to leading order in δ . This equation nicely relates the slope of the potential V_{ϕ} along the tangential direction T^a with its counterpart V_N along the normal direction N^a .

⁴Current observations indicate that the order of such a reference parameter is given by the departure of the spectral index from unity $\delta \sim |n_{\mathcal{R}} - 1|$.

⁵Let us recall that the parameter η was originally introduced in the study of single-field slow-roll inflation (Liddle and Lyth, 1992) as $\eta = M_{\text{pl}}^2 V''/V$. Therefore, in order to compare the present results with those following the original convention, we must write $\eta = \eta_{\parallel} + \epsilon$.

5.3.2 Perpendicular dynamics

Let us now turn our attention to parameter η_\perp defined in (eq. 4.18). Notice that this parameter is *not* related to the slow-roll variation of any given background quantity A in the sense of (eq. 5.42) and therefore is not constrained to be of $\mathcal{O}(\delta)$. Moreover, (eq. 4.22) tells us that η_\perp may be large compared to δ provided that the radius of curvature κ is small compared to $\sqrt{2\epsilon}M_{\text{Pl}}$. It is important to recognise that the curved inflationary trajectory ($\kappa^{-1} \neq 0$) has its origin in both the shape of the scalar potential V and the geometry of the scalar manifold where the theory lives. In particular, since H and $\dot{\phi}_0$ are assumed to evolve slowly, we expect the flat inflationary trajectory to remain close to the locus of points minimising the heaviest direction N^a of the potential. In other words, to ensure a bending of the trajectory we consider models where the potential is such that

$$V_{NN} \gg |\nabla_\phi V_\phi|. \quad (5.47)$$

It is entirely clear that in the event that the inflationary trajectory is suffering a turn, it will not coincide exactly with curve minimising the heaviest direction, which is made explicit by the result $V_N = \eta_\perp \dot{\phi}_0 H$ found in (eq. 4.18). It is in fact easy to show that the departure Δ from the real minima $V_N|_{\text{min}} = 0$ is roughly given by the condition $V_N + M^2 \Delta \simeq 0$, with M^2 given by (eq. 5.33). Then, with the help of (eq. 4.18) one finds that the ratio between the deviation Δ and the radius of curvature κ is given by

$$\frac{\Delta}{\kappa} \simeq \eta_\perp^2 \frac{H^2}{M^2}. \quad (5.48)$$

Observe that Δ/κ is essentially the combination $e^\beta - 1$ defined in (eq. 5.36) in the regime $k^2 \ll a^2 H^2$. Thus the parameter β appearing in the effective theory deduced in section 5.2.2 is giving us information regarding the dynamics perpendicular to the inflaton trajectory.

It is important to check whether the bending interferes with the flatness of the potential as felt by the adiabatic mode v^T . Observe from (eq. 5.8) and (eq. 5.11) that the effective mass $m^2(\tau)$ of v^T is given by

$$m^2(\tau) \equiv \Omega_{TT} - \zeta^2 \approx -a^2 H^2 (2 + 2\epsilon - 3\eta_\parallel), \quad (5.49)$$

where we have neglected terms of $\mathcal{O}(\delta^2)$. Note that $m^2(\tau) = \Omega_0(\tau)$, where $\Omega_0(\tau)$ is the effective mass encountered in the effective theory deduced in section 5.2.2. Thus, we see that η_\perp does not directly spoil the flatness of the potential V . Of course, one should explicitly verify in which way a bending affects the value of ϵ and η_\parallel by

examining the evolution of the background. We however point out that there is no reason *a priori* that fast and sudden turns with large values of η_\perp are not possible while staying in the slow-roll regime.

5.3.3 Equations of motion in the slow-roll regime

Putting all of the previous results together back into the set of equations (eq. 5.8) and (eq. 5.9), and neglecting terms of $\mathcal{O}(\delta^2)$, we finally arrive at the following equations of motion for the perturbations v_α^T and v_α^N :

$$\frac{d^2 v_\alpha^T}{d\tau^2} + 2aH\eta_\perp \frac{dv_\alpha^N}{d\tau} + a^2 H^2 \left(\frac{k^2}{a^2 H^2} - 2 - 2\epsilon + 3\eta_\parallel \right) v_\alpha^T + 2a^2 H^2 \eta_\perp (2 - \xi_\perp) v_\alpha^N = 0, \quad (5.50)$$

$$\frac{d^2 v_\alpha^N}{d\tau^2} - 2aH\eta_\perp \frac{dv_\alpha^T}{d\tau} + a^2 H^2 \left(\frac{k^2}{a^2 H^2} + \frac{M^2}{H^2} - 2 + \epsilon - \eta_\perp^2 \right) v_\alpha^N + 2a^2 H^2 \eta_\perp v_\alpha^T = 0, \quad (5.51)$$

where ξ_\perp was defined in (eq. 5.14). In the next section we deal with these equations numerically for suitable choices of the background parameters, and compare the obtained power spectrum with that of the effective theory obtained in section 5.2.2. We shall see how features in the power spectrum appear as a consequence of curved inflationary trajectory. We will, however, first give another derivation of the effective theory presented in section 5.2.2.

5.3.4 Effective theory for the adiabatic mode

In this section we offer another deduction of the effective theory shown in section 5.2.2. We begin by writing the action (eq. 4.49) for the particular case of two fields:

$$\begin{aligned} S = & \int d\tau d^3x \frac{1}{2} \left[\left(\frac{dv^T}{d\tau} \right)^2 - (\nabla v^T)^2 - (\Omega_{TT} - \zeta^2) (v^T)^2 \right] \\ & + \int d\tau d^3x \frac{1}{2} \left[\left(\frac{dv^N}{d\tau} \right)^2 - (\nabla v^N)^2 - (\Omega_{NN} - \zeta^2) (v^N)^2 \right] \\ & - \int d\tau d^3x v^N \left(\Omega_{TN} - \frac{d\zeta}{d\tau} - 2\zeta \frac{d}{d\tau} \right) v^T. \end{aligned} \quad (5.52)$$

Given that $\Omega_{NN} \gg |\Omega_{TT}|$ and $\Omega_{NN} \gg |\Omega_{TN}|$ the field v^N is the heavier of the two. Taking this scale as the scale of the heavy physics that we wish to integrate out, we

can formally evaluate the functional integral for v^N to obtain the one loop effective action for v^T as

$$S = \int d\tau d^3x \frac{1}{2} \left[\left(\frac{dv^T}{d\tau} \right)^2 - (\nabla v^T)^2 - (\Omega_{TT} - \zeta^2) (v^T)^2 \right] + \frac{1}{2} \int d\tau d^3x \int d\tau' d^3x' \mathcal{O}(\tau) v^T(\mathbf{x}, \tau) G(\mathbf{x}, \tau; \mathbf{x}', \tau') \mathcal{O}(\tau') v^T(\mathbf{x}', \tau') + S_{CT}, \quad (5.53)$$

with \mathcal{O} given by

$$\mathcal{O}(\tau) \equiv - \left(\Omega_{TN} - \frac{d\zeta}{d\tau} - 2\zeta \frac{d}{d\tau} \right), \quad (5.54)$$

and the Green's function G given by

$$G(x, \tau; x', \tau') = \frac{1}{\square + \Omega_{NN} - \zeta^2}. \quad (5.55)$$

The term S_{CT} renormalises the effective action for the background inflaton field. We have to demand that the parameters of this effective action that satisfy the slow-roll conditions rather than those of the bare action (Burgess et al., 2010), which we presume to be the case here. In general, evaluating the full effective action is a highly non-trivial task. However, in Fourier space one can formally make the expansion

$$G(\tau, \tau', k) = \frac{1}{-\partial_\tau^2 + k^2 + \Omega_{NN} - \zeta^2} = \frac{1}{\omega^2} \left(1 - \frac{\partial_\tau^2}{\omega^2} + \dots \right), \quad (5.56)$$

where

$$\omega^2 \equiv k^2 + \Omega_{NN} - \zeta^2. \quad (5.57)$$

Where implicit in the above is that if the scale M tends to the cutoff of the theory (so that $V_{NN} \sim M^2$) we can neglect the temporal derivatives in the expansion above, relative to the mass term and the spatial derivatives (which always become significant at horizon crossing). This reduces the Green's function to leading order of only the contact term.⁶ Integrating the second term in (5.53) by parts results in

$$S = \int d\tau d^3k \frac{1}{2} \left\{ \left(\frac{dv^T}{d\tau} \right)^2 e^{\beta(k, \tau)} - \left[k^2 + \bar{\Omega}(\tau, k) \right] (v^T)^2 \right\}, \quad (5.58)$$

⁶A related derivation for the effective field theory of the inflaton field coupled to a massive field with a cubic interaction term with the inflaton can be found in Rubin (2001).

with

$$e^{\beta(\tau, k^2)} \equiv 1 + 4\eta_{\perp}^2 \left(\frac{M^2}{H^2} - 2 + \epsilon - \eta_{\perp}^2 + \frac{k^2}{a^2 H^2} \right)^{-1}, \quad (5.59)$$

$$\bar{\Omega}(\tau, k) \equiv \Omega_0 - \frac{4a^4 H^4 \eta_{\perp}^2 (1 + \epsilon - \eta_{\parallel})^2}{\omega^2} + 4 \frac{d}{d\tau} \left[\frac{a^3 H^3 \eta_{\perp}^2 (1 + \epsilon - \eta_{\parallel})}{\omega^2} \right], \quad (5.60)$$

whilst Ω_0 is given by (eq. 5.40). Making the field redefinition $\varphi \equiv e^{\beta/2} v^T$ (and upon integrating by parts the resulting friction term), one then obtains the effective action

$$S = \int d\tau d^3k \frac{1}{2} \left[\left(\frac{d\varphi}{d\tau} \right)^2 - \varphi e^{-\beta(\tau, k)} k^2 \varphi - \varphi \Omega(\tau, k) \varphi \right], \quad (5.61)$$

where $\Omega(\tau, k^2)$ is defined as in (eq. 5.39). We thus see that the expression (eq. 5.41) follows.

5.4 Features in the power spectrum

We now study the evolution of perturbations and analyse how features in the primordial spectrum are generated along curved trajectories. To this extent, we solve (eqs. 5.50 and 5.51) numerically for different background solutions representing curved trajectories and obtain the mode solutions v_{α}^I which, with the help of (eq. 5.29), provide us the desired power spectrum at the end of inflation. For definiteness, we consider models of inflation with an inflationary period of at least 60 e -folds and set the initial conditions a few e -folds before this period starts. To avoid unnecessary complications with initial conditions, we considered models where turns in the trajectory only happen within the last 60 e -folds. Before this period, $\eta_{\perp} = 0$ and the equations of motion determining the evolution of perturbations reduce to

$$\frac{d^2 v_{\alpha}^T}{d\tau^2} + a^2 H^2 \left(\frac{k^2}{a^2 H^2} - 2 - 2\epsilon + 3\eta_{\parallel} \right) v_{\alpha}^T = 0, \quad (5.62)$$

$$\frac{d^2 v_{\alpha}^N}{d\tau^2} + a^2 H^2 \left(\frac{k^2}{a^2 H^2} + \frac{M^2}{H^2} - 2 + \epsilon \right) v_{\alpha}^N = 0. \quad (5.63)$$

Then, as long as ϵ and η_{\parallel} are small, we are allowed to make use of initial conditions (eq. 4.65-4.67) with $e_{\alpha}^l = \delta_{\alpha}^l$, and $v_1(k)$ and $v_2(k)$ given by

$$v_1(k) = \frac{\sqrt{\pi}}{4\sqrt{a_i H_i}} e^{i\frac{\pi}{2}(\nu_1 + \frac{1}{2})} H_{\nu_1}^{(1)}\left(\frac{k}{a_i H_i}\right), \quad (5.64)$$

$$v_2(k) = \frac{\sqrt{\pi}}{4\sqrt{a_i H_i}} e^{i\frac{\pi}{2}(\nu_2 + \frac{1}{2})} H_{\nu_2}^{(1)}\left(\frac{k}{a_i H_i}\right), \quad (5.65)$$

where $H_{\nu}^{(1)}(x)$ denotes the first kind Hankel function, whereas a_i and H_i are the values for the scale factor and Hubble parameter at the initial time τ_i . Similarly, the quantities $\pi_1(k)$ and $\pi_2(k)$ entering the initial conditions (eq. 4.67) are given by the time derivatives of the previous expressions. On the other hand, the parameters ν_1 and ν_2 are respectively given by

$$\nu_1 = \sqrt{\frac{(3 - \epsilon)^2}{4(1 - \epsilon)^2} - 3(\eta - \epsilon)}, \quad (5.66)$$

$$\nu_2 = \sqrt{\frac{(3 - \epsilon)^2}{4(1 - \epsilon)^2} - \frac{M^2}{H_i^2}}. \quad (5.67)$$

Note that in the short wavelength limit, $k \gg a_i H_i$, the previous conditions matches the mode fluctuations about a Bunch-Davies vacuum (eq. 4.70), discussed in section 4.3.2. In all of the cases examined, we consider inflationary trajectories where ϵ , η_{\parallel} and ξ_{\parallel} remain small during the interval of interest, while allowing different types of time variation of η_{\perp} , which is the quantity that parametrises the bending.

5.4.1 Constant radius of curvature

Let us start by considering the simple case in which η_{\perp} is constant during the whole period of inflation where currently accessible modes were generated. As we have already emphasised, if ϵ remains nearly constant a constant η_{\perp} corresponds to a trajectory with a constant radius of curvature κ . We find that the overall effect of having a constant turn is simply to normalise the amplitude of the spectrum, without modifying the usual single-field dependence of the spectral index $n_{\mathcal{R}}$ in terms of the slow-roll parameters ϵ and η_{\parallel} (see also Chen and Wang, 2010a,b),

$$n_{\mathcal{R}} - 1 = 2\eta_{\parallel} - 4\epsilon. \quad (5.68)$$

In the case $M^2/H^2 \gg 1$, the predicted power spectrum obtained by the effective theory is indistinguishable from the one obtained by solving the full set of equations.

Moreover, with the help of this effective theory, it is in fact possible to infer a simple relation between the power spectrum $\mathcal{P}_{\mathcal{R}}(k)$ with $\eta_{\perp} \neq 0$ and the analytical power spectrum $\mathcal{P}_{\mathcal{R}}^{(0)}(k)$ computed with $\eta_{\perp} = 0$. To this extent, notice that although $\beta(k, \tau)$ is a function of k , we see that when the physical wavelength of the mode becomes larger than the scale M^{-1} (i.e. $k^2/a^2 \leq M^2$), the parameter $\beta(\tau, k)$ becomes effectively k independent, and we can write

$$e^{\beta} = 1 + 4\eta_{\perp}^2 \frac{H^2}{M^2}. \quad (5.69)$$

Since $M^2 \gg H^2$, this happens before horizon crossing and the relevant dynamics is well described by this k -independent form of β . Then the relation between $\mathcal{P}_{\mathcal{R}}(k)$ and $\mathcal{P}_{\mathcal{R}}^{(0)}(k)$, as predicted by the effective theory, becomes

$$\mathcal{P}_{\mathcal{R}}(k) = \left(1 + 4\eta_{\perp}^2 \frac{H^2}{M^2}\right) \mathcal{P}_{\mathcal{R}}^{(0)}(k). \quad (5.70)$$

This result modifies the usual normalisation condition of the spectrum coming from the COBE data, leading to the following relation among the various parameters:

$$\left(1 + 4\eta_{\perp}^2 \frac{H^2}{M^2}\right) \mathcal{P}_{\mathcal{R}}^{(0)}(k_{\text{COBE}}) \approx 2.46 \times 10^{-9}. \quad (5.71)$$

Physically, this result may be interpreted as coming from the fact that heavy and light modes are interchanging energy at a constant rate, therefore rendering only a change in the overall amplitude of the spectrum. However, as manifest from the effective theory (eq. 5.38), the speed of sound is modified as

$$c_s^2 = e^{-\beta} = \left(1 + 4\eta_{\perp}^2 \frac{H^2}{M^2}\right)^{-1}. \quad (5.72)$$

This implies the generation of nongaussianity noticeable in the bispectrum, as studied in Chen and Wang (2010a,b).

5.4.2 Single turn in the trajectory

As a next step, we consider the presence of a single turn in the inflationary trajectory. To simplify our analysis, we consider the specific case in which the trajectory is initially autoparallel to a geodesic (a straight path), then goes through a short period in which it suffers a turn, and finally goes back to the curve autoparallel to a geodesic. Figure 5.2 shows a prototype example of such a situation. We also assume

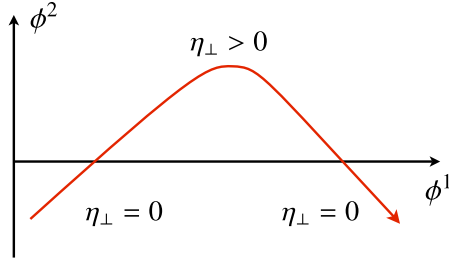


Figure 5.2: The figure shows a prototype example of a trajectory which suffers a localised bend towards the right.

that throughout this process all the slow-roll parameters except for η_{\perp} remain nearly constant. To model this situation, we take η_{\perp} to be an analytical function of the e -fold number N in the following way:

$$\eta_{\perp}(N) = \frac{\eta_{\perp\max}}{\cosh^2 [2(N - N_0)/\Delta N]}, \quad (5.73)$$

where ΔN is the number of e -folds during which the bending happens, and N_0 is the e -fold value at which the bending is at its peak, in which case $\eta_{\perp}(N_0) = \eta_{\perp\max}$. We recall that N may be suitably defined from conformal time τ through the relation $dN = aHd\tau$. For the other slow-roll parameters we choose the reference values $\epsilon = 0.022$ and $\eta_{\parallel} = 0.034$. These values correspond to a spectral index $n_{\mathcal{R}} = 0.98$ and to a tensor to scalar ratio $r = 0.35$, which are marginally compatible with current CMB tests (Larson et al., 2010). Additionally, these values imply $H = 10^{-5} M_{\text{Pl}}$. Figure 5.3 shows the power spectra for six cases with different choices of the parameters ΔN , $\eta_{\perp\max}$ and M^2 . The plots contain both the spectrum obtained by solving the full coupled system of equations (solid line) and the spectrum obtained by solving the effective single-field equation of motion (dashed line). For simplicity, we normalise our results in units of 2.46×10^{-9} and give the scale k in units of Mpc^{-1} . As a reference, we have included the case $\eta_{\perp} = 0$, which corresponds to the power spectrum that would be obtained in the single-field case.

The main characteristic shown by the plots are oscillatory features appearing in the spectrum. It may be noticed that the e -fold width ΔN during which the turn takes place actually set the scale k of the oscillatory features. On the other hand, the amplitude of the oscillations is roughly dictated by the ratio $4\eta_{\perp\max}H^2/M^2$. More precisely, the amplitude of the largest oscillatory feature is of order $\delta\mathcal{P}_{\mathcal{R}}/\mathcal{P}_{\mathcal{R}} \sim 4\eta_{\perp\max}H^2/M^2$, which agrees with the result of (eq. 5.70). Additionally, the match between the curve

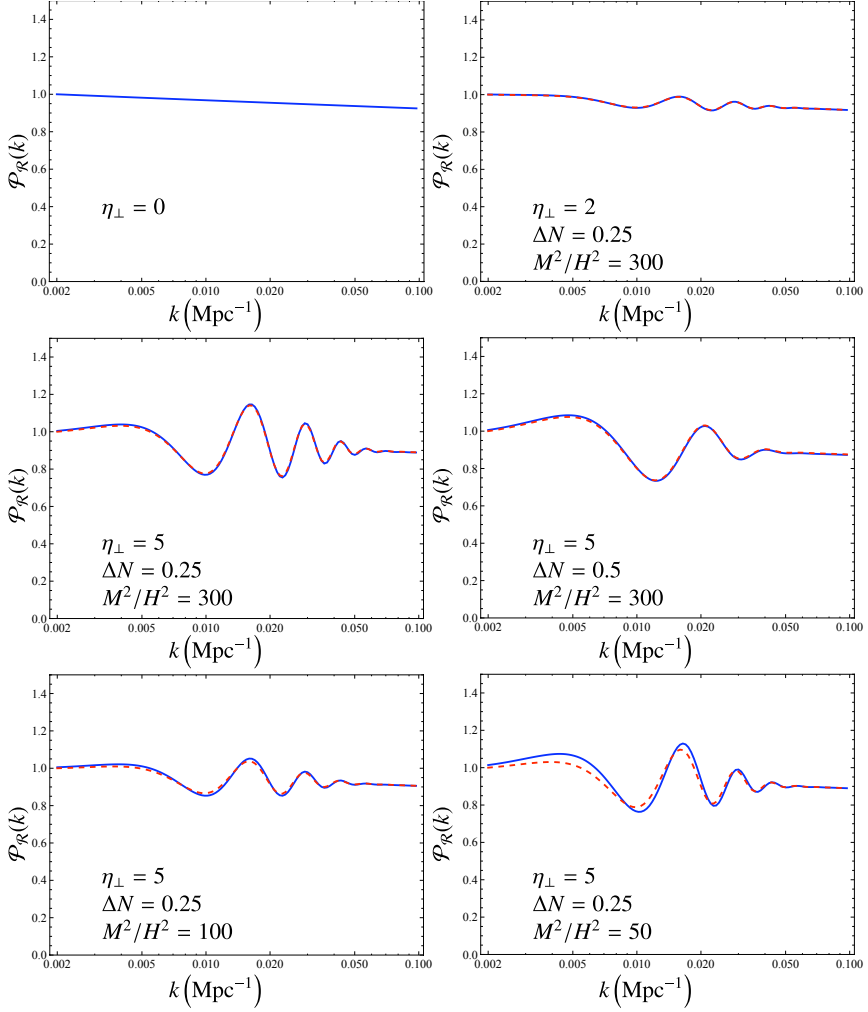


Figure 5.3: The primordial power spectrum $\mathcal{P}_R(k)$ normalised in units of 2.46×10^{-9} , obtained for six different choices of ΔN , $\eta_{\perp, \text{max}}$ and M^2 . The plots show a comparison between the power spectrum obtained using the full system of equations (solid line) and the one obtained using the effective theory (dashed line). We have chosen as a pivot scale the value $k_* = 0.002 \text{Mpc}^{-1}$.

predicted by the effective theory and the full set of equations becomes better as M^2/H^2 acquires larger values, irrespective of how large is β . In fact, in all of the examples shown we have $\beta \sim 1$.

The appearance of oscillatory features, not just a single bump, in the spectrum reflects the fact that both modes v^N and v^T backreact at sub-horizon scales as the turn happens. Once both modes cross the horizon, the amplitude of the adiabatic mode becomes frozen (therefore capturing the moment in which the mode was receiving or releasing energy) while the amplitude of the heavy mode quickly decays due to the accelerated expansion. In fact, we have checked that the levels of isocurvature perturbations at the end of inflation are negligible.

5.4.3 A specific example

As a last step towards understanding the effects of curved trajectories, we discuss our results applied to a specific toy model, where turns are produced due to the non-trivial evolution of the sigma model metric. Let us consider a two-field model with fields $\phi^1 = \chi$ and $\phi^2 = \psi$ with a kinetic term containing the following sigma model metric:

$$\gamma_{ab} = \begin{pmatrix} 1 & \Gamma(\chi) \\ \Gamma(\chi) & 1 \end{pmatrix}, \quad (5.74)$$

where $\Gamma(\chi)$ is only a function of the χ field and restricted to satisfy $\Gamma^2(\chi) < 1$. The non-vanishing connections are $\Gamma_{\chi\chi}^\chi = -\Gamma_\chi/(1 - \Gamma^2)$ and $\Gamma_{\chi\chi}^\psi = \Gamma_\chi/(1 - \Gamma^2)$ with $\Gamma_\chi = \partial_\chi \Gamma$, and the equations of motion for the background fields are found to be

$$\ddot{\chi} - \frac{\Gamma\Gamma_\chi}{1 - \Gamma^2}\dot{\chi}^2 + 3H\dot{\chi} + \frac{1}{1 - \Gamma^2}V_\chi - \frac{\Gamma}{1 - \Gamma^2}V_\psi = 0, \quad (5.75)$$

$$\ddot{\psi} + \frac{\Gamma_\chi}{1 - \Gamma^2}\dot{\chi}^2 + 3H\dot{\psi} + \frac{1}{1 - \Gamma^2}V_\psi - \frac{\Gamma}{1 - \Gamma^2}V_\chi = 0, \quad (5.76)$$

where $V_\chi = \partial_\chi V$ and $V_\psi = \partial_\psi V$. For concreteness, let us consider the following separable scalar field potential:

$$V(\chi, \psi) = V_0(\chi) + \frac{1}{2}M^2\psi^2. \quad (5.77)$$

In the particular case of $\Gamma = 0$, the dynamics of the two fields decouple and inflation may be achieved with χ by a suitable choice of the potential $V_0(\chi)$. If, however, $\Gamma(\chi)$ is allowed to be non-vanishing for certain values of χ , then a mixing between the two modes is inevitable, and the inflationary trajectory will be curved. Following

the discussion at the beginning of Section 5.2, we choose the tangential and normal vectors T^a and N^a as in (eq. 5.4) and (eq. 5.5):

$$T^a = \frac{1}{\dot{\phi}_0} (\dot{\chi}, \dot{\psi}), \quad (5.78)$$

$$N^a = \frac{1}{\dot{\phi}_0 \sqrt{1 - \Gamma^2}} (-\dot{\psi} - \Gamma \dot{\chi}, \dot{\chi} + \Gamma \dot{\psi}), \quad (5.79)$$

where $\dot{\phi}_0 = \dot{\chi}^2 + \dot{\psi}^2 + 2\Gamma \dot{\chi} \dot{\psi}$. Recall that with this convention η_\perp is allowed to change its sign. The relevant background parameters describing this situation are then

$$\epsilon = \frac{\dot{\chi}^2 + \dot{\psi}^2 + 2\Gamma \dot{\chi} \dot{\psi}}{2M_{\text{pl}}^2 H^2}, \quad (5.80)$$

$$\eta_\parallel = 3 + \frac{\dot{\chi} V_\chi + \dot{\psi} V_\psi}{H (\dot{\chi}^2 + \dot{\psi}^2 + 2\Gamma \dot{\chi} \dot{\psi})}, \quad (5.81)$$

$$\eta_\perp = -\frac{(\dot{\psi} + \Gamma \dot{\chi}) V_\chi - (\dot{\chi} + \Gamma \dot{\psi}) V_\psi}{H \sqrt{1 - \Gamma^2} (\dot{\chi}^2 + \dot{\psi}^2 + 2\Gamma \dot{\chi} \dot{\psi})}, \quad (5.82)$$

where H is given by $6M_{\text{pl}}^2 H^2 = \dot{\chi}^2 + \dot{\psi}^2 + 2\Gamma \dot{\chi} \dot{\psi} + 2V$. For concreteness, let us consider a parameter $\Gamma(\chi)$ having the following χ -dependence:

$$\Gamma(\chi) = \frac{\Gamma_0}{\cosh^2 [2(\chi - \chi_0)/\Delta\chi]}, \quad (5.83)$$

where Γ_0 is the maximum value attained by $\Gamma(\chi)$. We take the potential $V_0(\chi)$ as

$$V_0(\chi) = \frac{1}{256V_0^5} \left(16V_0^3 + V_1^2 \chi^3 - 2V_0 V_1 \chi^2 (V_1 + 2V_2 \chi) + 8V_0^2 \chi (V_1 + \chi(V_2 + V_3 \chi)) \right)^2, \quad (5.84)$$

with $V_0 = 3H_i$, $V_1 = -\sqrt{2\epsilon_i} V_0$, $V_2 = V_0(\epsilon_i + \eta_i)$ and $V_3 = 10^{-4} V_0$, where, as before, H_i , ϵ_i and η_i render values $\epsilon = 0.022$ and $\eta_\parallel = 0.034$ for the slow-roll parameters in the absence of curves. For this specific configuration, we found that the background value of $\epsilon(\tau)$ remains nearly constant at the attractor value $\epsilon = 0.022$ whereas the background value of $\eta_\parallel(\tau)$ is more sensitive to the turns suffered by the trajectory, having small deviations from the attractor value $\eta_\parallel = 0.034$. Additionally, we found two relevant time scales determining the behaviour of background quantities η_\parallel and η_\perp :

$$T_\psi \equiv M^{-1}, \quad (5.85)$$

$$T_\chi \equiv \frac{\Delta\chi}{\dot{\phi}_0} = \frac{\Delta\chi}{\sqrt{2\epsilon} M_{\text{pl}} H}. \quad (5.86)$$

The appearance of these time scales are actually easy to understand. First, notice that T_χ is the time during which the turn takes place whereas T_ψ is the oscillation period of the massive field ψ . We find that if $T_\chi \ll T_\psi$, then the background dynamics is such that $\phi_0^a = (\chi, \psi)$ oscillates about $\psi = 0$, meaning that both η_{\parallel} and η_{\perp} presented oscillatory features with frequency $O(T_\psi^{-1})$. On the other hand, if $T_\chi \gg T_\psi$, the background field departs adiabatically from the minima of the potential $\psi = 0$, and the time evolution of η_{\parallel} and η_{\perp} is dictated by the time scale T_χ . This latter case may be interpreted as a situation where the trajectory is momentarily pushed towards one of the walls of the potential, as the curve takes place. Figure 5.4 shows the background values of η_{\perp} and η_{\parallel} (as functions of the e -fold number N) for the case $\Gamma_0 = 0.9$, $M^2 = 300H^2$ and two values of $\Delta\chi$, namely $\Delta\chi = 0.076M_{\text{Pl}}$ and $\Delta\chi = 0.041M_{\text{Pl}}$. In the latter case, it may be appreciated how the time scale T_ψ appears mildly in the shape of η_{\perp} .

The figure also shows the power spectrum obtained for the two described cases (right panels). In the present examples, the features appearing in the spectrum are not as regular as those of Figure 5.3. This is mainly because in the present situation the curvilinear trajectory contains several turns, in order to go back to the attractor solution. Although in this specific model the slow-roll parameter η_{\parallel} appears to be sensitive to the mass scale M and the curves taking place, it is important to notice that this is a model dependent characteristic, and that in general η_{\parallel} may show various types of behaviour depending on the sigma model metric and the potential. In general, however, the momentary time variation of η_{\parallel} due to curved trajectories does not spoil the slow-roll regime, and background fields tend to quickly evolve back to the attractor behaviour characteristic of the single-field case as soon as the bending of the trajectory stops. In this regard, we find that the time variation of η_{\parallel} is not relevant for the appearance of features in the power spectrum, and that the main contribution is coming from the derivative interactions due to η_{\perp} in the equations of motion.

5.4.4 Enhancement of nongaussianity

We briefly elaborate here on another potentially observable feature which is so far not discussed. In the previous section the power spectrum of the curvature perturbation was computed for a few examples where the inflaton traverses sufficiently curved regions in field space. From the results, it is clear that features in the spectrum will be generated each time the trajectory traverses a bend. These features are produced via the kinetic interaction between the heavy isocurvature modes and the light curvature mode as the turns are traversed by the background field. Crucially, in these examples the heavy mode remained very massive throughout ($M^2 \gg H^2$), highlighting the

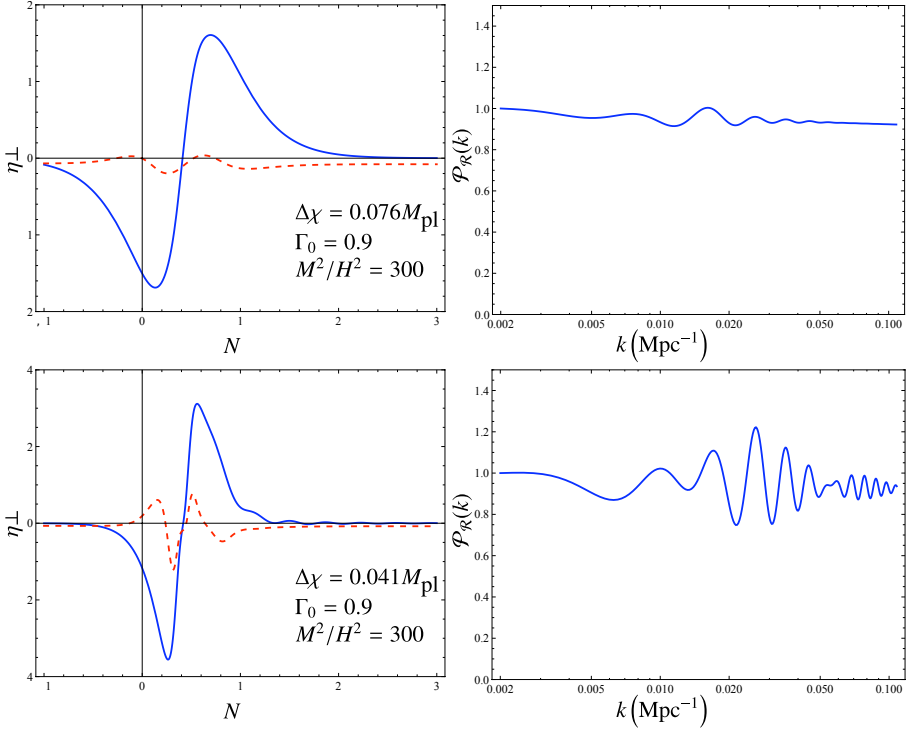


Figure 5.4: Left panels: the evolution of η_\perp (solid line) and $10 \times \eta_\parallel$ (dashed line) as functions of e -fold number N for two set of values of parameters $\Delta\chi$, Γ_0 and M^2/H^2 . In the first case, $\Delta\chi = 0.076 M_{\text{pl}}$ and the maximum value of η_\perp is about $|\eta_\perp| \approx 1.7$, whereas in the second case, $\Delta\chi = 0.041 M_{\text{pl}}$ and the maximum value becomes $|\eta_\perp| \approx 3.5$. Right panels: the resulting primordial power spectrum $\mathcal{P}_R(k)$, normalised in units of 2.46×10^{-9} , obtained for the set of parameters used in the plots of η_\perp . The scale k appears in units of Mpc^{-1} .

fact that heavy fields may not always be disregarded (truncated) when computing the spectrum for adiabatic modes.

What is important to note is that the interaction between curvature and isocurvature modes implies a change in the speed of sound for the curvature perturbations – as long as $M^2 \gg H^2$, $\beta(\tau, k)$ is effectively k -independent before horizon crossing and

the speed of sound may be written as

$$c_s^2 = e^{-\beta} = \left(1 + 4\eta_{\perp}^2 \frac{H^2}{M^2}\right)^{-1}. \quad (5.87)$$

As is well known, a model with a speed of sound significantly smaller than unity gives rise to a noticeable level of nongaussianity of equilateral type, characterised by the non-linear parameter (Bartolo et al., 2004)

$$f_{\text{NL}}^{(\text{eq})} \sim \frac{1}{c_s^2}. \quad (5.88)$$

Thus, we are led to reason that for generic models of inflation with curvilinear trajectories in a multi-dimensional field space, glitches in the power spectrum are accompanied by a correlated enhancement of nongaussianity of the equilateral type, provided that the turns in the inflaton trajectory violate the adiabatic approximation vigorously enough – a phenomenon which we have argued occurs at various points in field space in many realistic realisations of inflation. Thus although there appear to be many models where either non-trivial modulations in the power spectrum (e.g. features in the single-field inflaton potential, Starobinsky, 1992, Adams et al., 2001, Tocchini-Valentini et al., 2005, Gong, 2005, Covi et al., 2006, Hunt and Sarkar, 2007, Ichiki et al., 2010, Peiris and Verde, 2010, Hamann et al., 2010) or large equilateral nongaussianity (e.g. DBI inflation, Silverstein and Tong, 2004, Alishahiha et al., 2004) result, it appears that in generic multi-field models with curved inflationary trajectories, both are present and correlated. Evidently, the effective quadratic action (eq. 5.41) contains the leading higher order corrections which can also result in non-Gaussian signatures and implies the non-linear parameter (eq. 5.88) (Cheung et al., 2008). However, to fully describe the bispectrum associated with the curvature perturbation, we need to properly take into account the cubic order action including gravity. We will discuss this issue in a separate publication.

5.5 Conclusions

Multi-field models of inflation contain a range of physics which goes beyond that encountered within the single-field paradigm. In this work we have focused on the particular case where all of the scalar fields remain massive during inflation except for one, which slowly rolls down the multi-field potential. We have found that curved inflationary trajectories can generate significant features in the primordial spectrum of

density perturbations arising from normal modes becoming excited and backreacting on the dynamics of the adiabatic mode.

To achieve these results, an extension of Groot Nibbelink and van Tent (2000, 2002), we analysed the evolution of the quantum perturbations of a general multi-field setup, including the presence of a non-canonical kinetic term. Our methods are completely general and naturally incorporate those implemented in previous works (Lalak et al., 2007b, Tsujikawa et al., 2003), where stochastic Gaussian variables are used. Moreover, although the main focus of this work was the study of systems where there exists a hierarchy, our results may be used to study a wide range of situations, including situations where no such hierarchies are present.

Our formalism allows us to consider time-dependent situations beyond the regime of applicability of existing methods, such as inflaton trajectories with fast, sudden turns (regardless of whether the sigma model metric is canonical or non-canonical) as well as more general situations in which the masses of the heavy fields in the orthogonal direction are changing along the trajectory (even if they still remain much heavier than H^2 and all other scales of interest). Additionally, we wish to emphasise that these non-decoupling effects have their origin in the non-geodesic nature of the trajectories in field space.⁷

Our results highlight the limitations of simply truncating heavy physics when modelling single-field realisations of inflation and show under which circumstances high energy effects can leave an imprint on the power spectrum. The main reason behind these effects is the existence of kinetic couplings between adiabatic and non-adiabatic modes, emerging as the inflationary trajectory suffers a turn. As we have seen in section 4.3.1, it is always possible to change basis to a canonical frame where such interactions are absent. In that case, the eigenvectors of the perturbation mass matrix quickly vary as the inflationary trajectory turns, and we are left with the alternative point of view by which these high energy effects appear due to a violation of the adiabatic condition for truncating heavy fields. In fact, if the heavy fields are sufficiently massive, we find that we can construct an effective field theory for the adiabatic modes encapsulating the relevant effects of the full multi-field dynamics. As we have seen, such effects are not mere corrections to the standard single-field theory, but represent entirely new contributions to the quadratic action for perturbations.

Particularly noteworthy is the presence of potentially observable signatures that result from a reduced speed of sound for the adiabatic perturbations during sudden turns. As a corollary, correlated nongaussianity will also become manifest as a result of these sudden turns although a full analysis studying the details of their appearance

⁷Recent work by Cremonini et al. (2010b) discusses some of these effects in a particular model, the so-called gelaton model of Tolley and Wyman (2010).

Chapter 5: Two-field models of inflation

in multi-field inflation is beyond the scope of this chapter and will be addressed in a future report. Nevertheless, it would appear that in generic multi-field models with curved inflationary trajectories, both effects are present and correlated, and can potentially give information about other, much heavier, fields that would otherwise be inaccessible to experiment.